## Supplementary Information

# Visible-light $CO_2$ photoreduction of polyoxometalate-based hybrids with different cobalt clusters

Wei Yao, Chao Qin,* Na Xu, Jie Zhou, Chunyi Sun, Li Liu* and Zhongmin Su

Key Laboratory of Polyoxometalate Science, Institute of Functional Material Chemistry, National & Local United Engineering Laboratory for Power Battery, Northeast Normal University, Changchun, Jilin, 130024, P. R. China

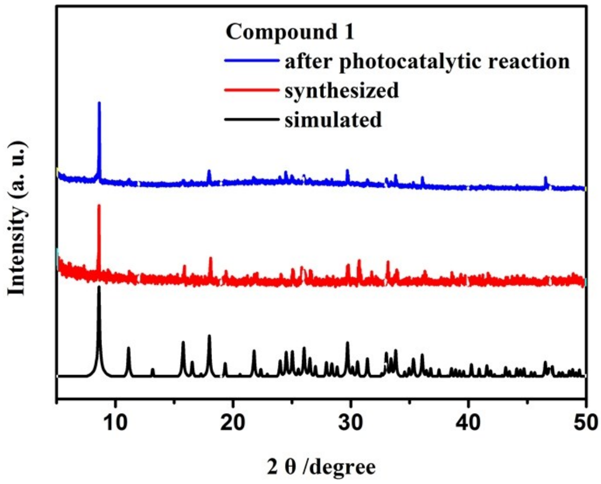


**Fig. S1** PXRD patterns of **1** with simulated (black line), as-synthesized (red line) and after photocatalytic reaction (blue line).

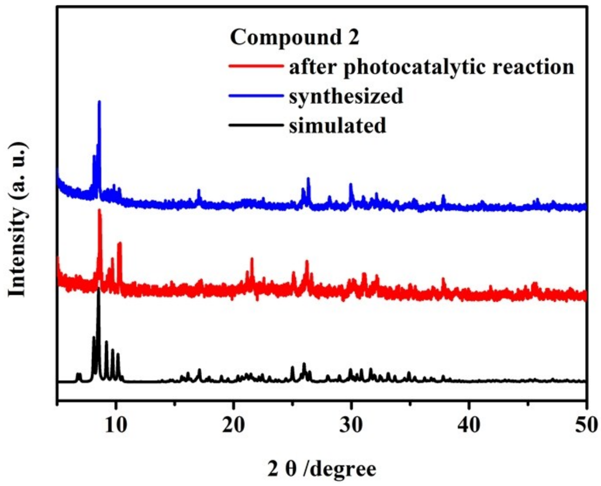


**Fig. S2** PXRD patterns of **2** with simulated (black line), as-synthesized (red line) and after photocatalytic reaction (blue line).

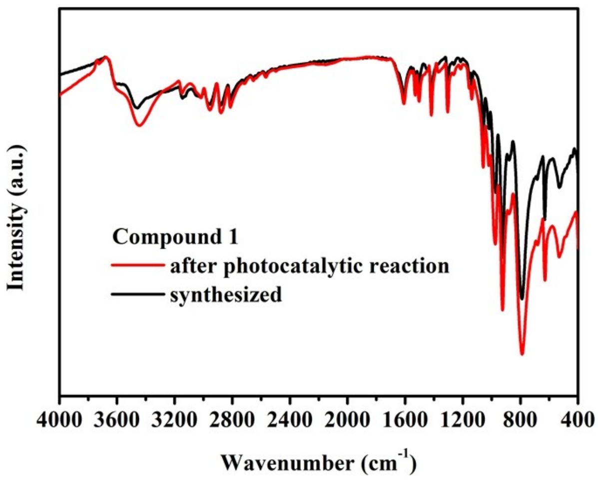


**Fig. S3** IR spectra of **1** with as-synthesized (black line) and after photocatalytic reaction (red line).

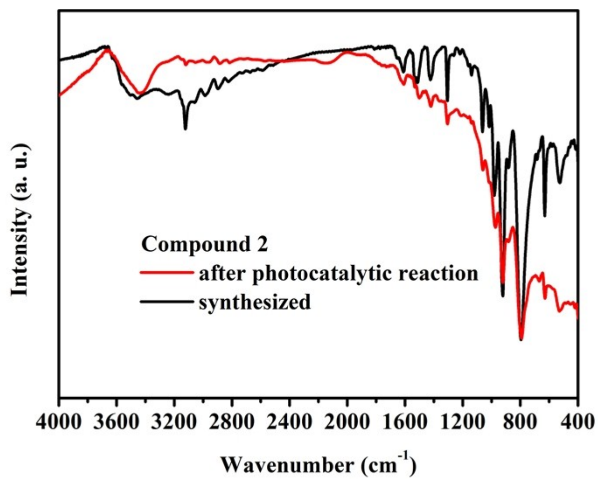


**Fig. S4** IR spectra of **2** with as-synthesized (black line) and after photocatalytic reaction (red line).

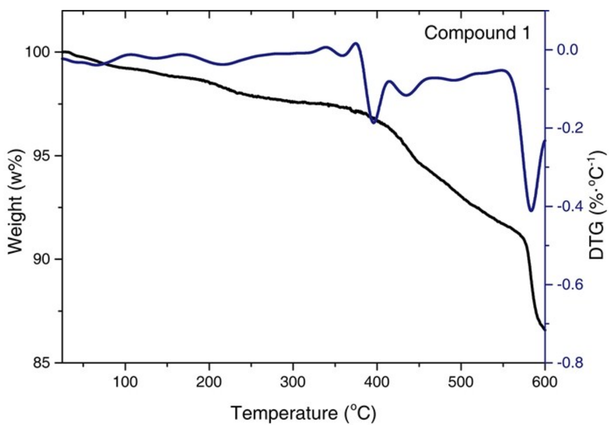


**Fig. S5** TG and DTG curves of compound **1**.

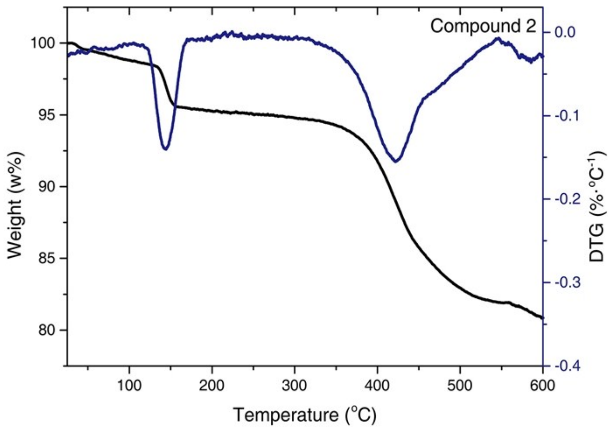


**Fig. S6** TG and DTG curves of compound **2**.

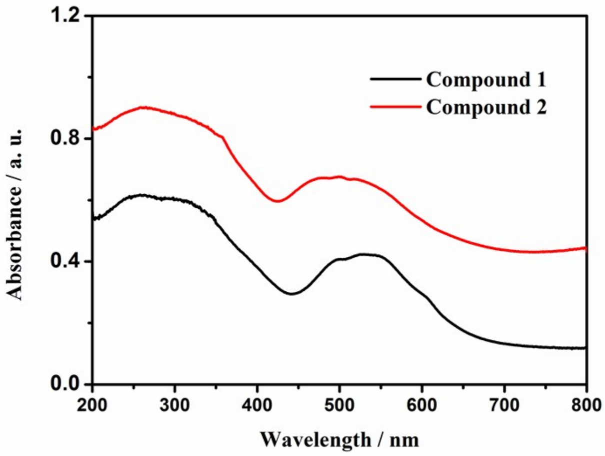


**Fig. S7** UV-Vis spectra of compounds **1** and **2**.

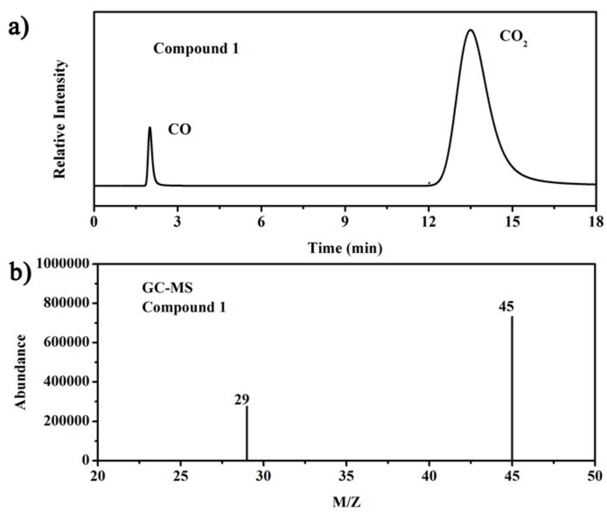


**Fig. S8** (a) Gas chromatogram and (b) mass spectra analyses of the carbon source of the evolved CO in the photocatalytic reduction of $^{13}CO_2$ by compound **1**.

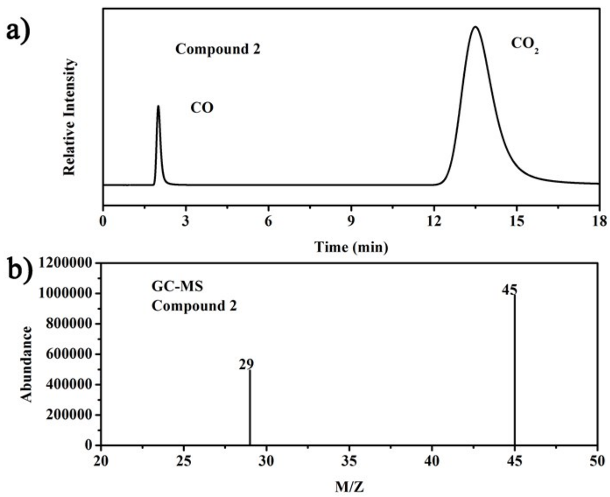


**Fig. S9** (a) Gas chromatogram and (b) mass spectra analyses of the carbon source of the evolved CO in the photocatalytic reduction of $^{13}CO_2$ by compound **2**.

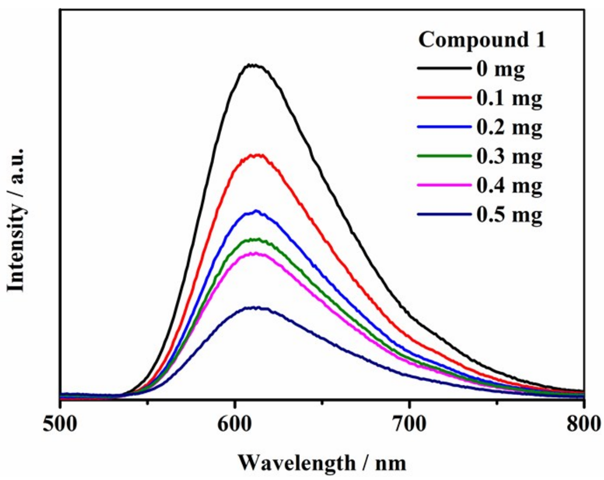


**Fig. S10** Emission specta of $[Ru(bpy)_3]Cl_2{\cdot}6H_2O$ ($1.0 \times 10^{-6}$ M) in $CH_3CN$ in the absence and presence of **1** (0.03 μM–0.15 μM); excitation wavelength: 452 nm.

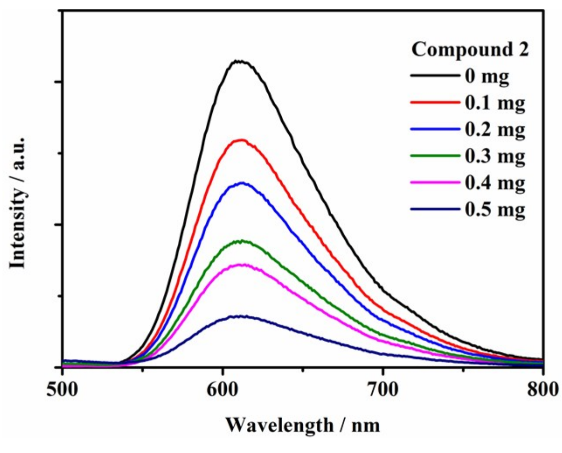


**Fig. S11** Emission spectra of $[Ru(bpy)_3]Cl_2{\cdot}6H_2O$ ($1.0 \times 10^{-6}$ M) in $CH_3CN$ in the absence and presence of **2** (0.03 μM–0.15 μM); excitation wavelength: 452 nm.

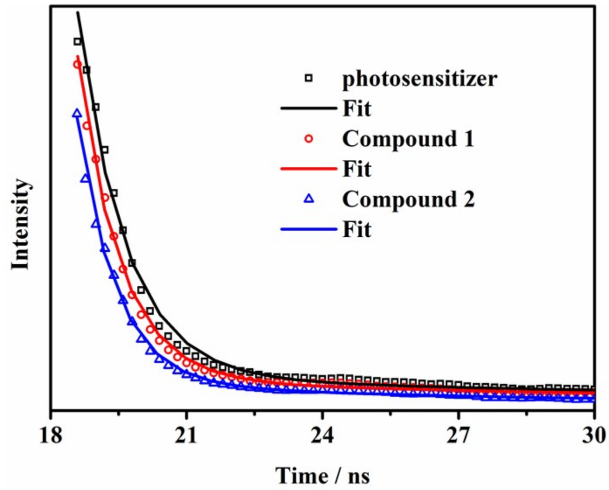


**Fig. S12** Transient PL decay of $[Ru(bpy)_3]Cl_2·6H_2O$ in $CH_3CN$ in the absence and presence of 0.5 mg **1** and 0.5 mg **2**.

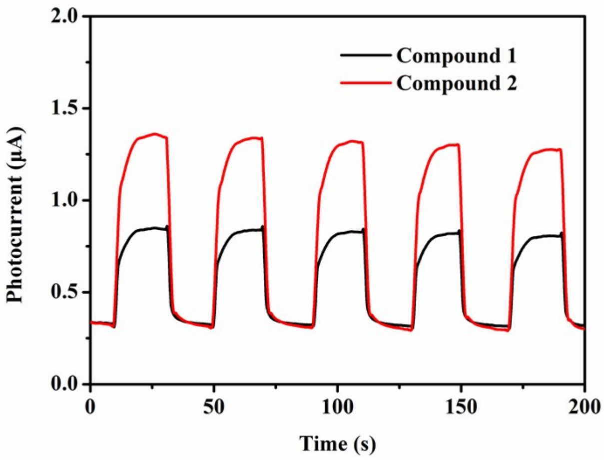


**Fig. S13** Transient photocurrent responses of compounds **1** and **2** under visible-light irradiation (λ≥420 nm).

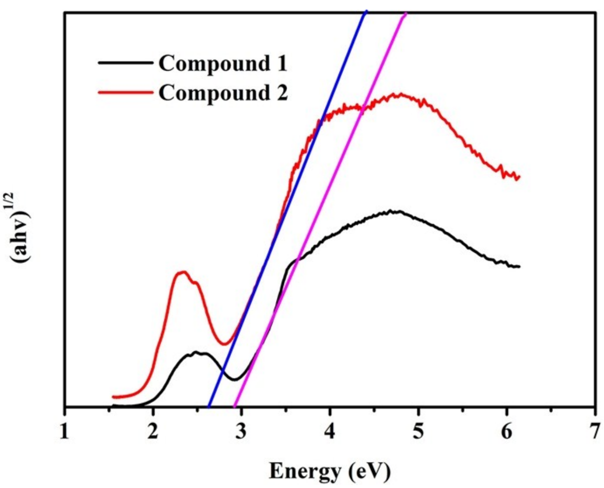


**Fig. S14** Tauc plot of $(\alpha h\nu)^{1/2}$ versus $h\nu$ derived from UV−vis spectrum in panel for band gap estimation. The horizontal (x) axis is the baseline, the pink line of **1** and the blue line of **2** are the tangent of the curve.

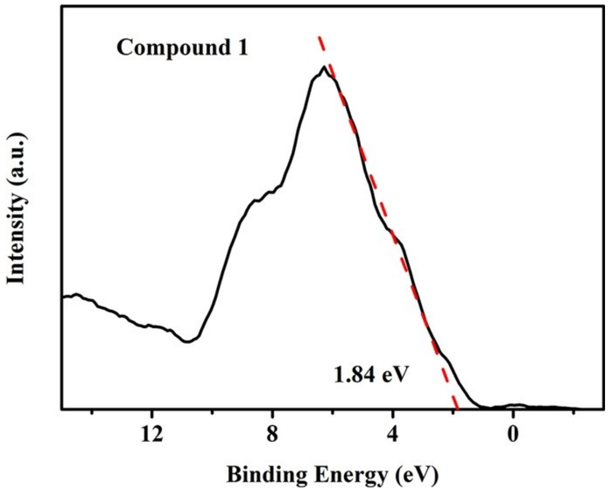


**Fig. S15** VB XPS spectrum for compound **1**.

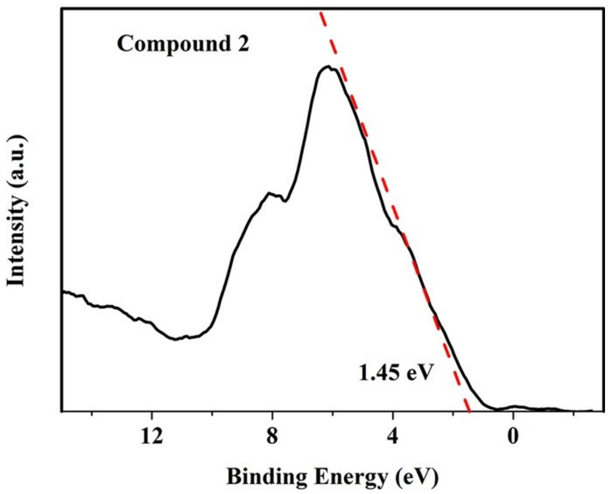


**Fig. S16** VB XPS spectrum for compound **2**.

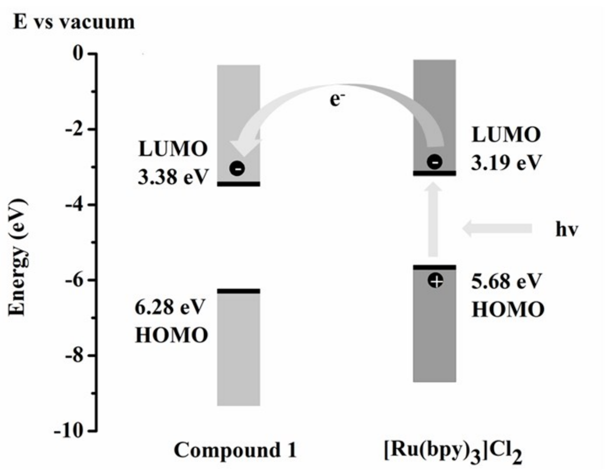


**Fig. S17** Schematic energy-level diagram showing electron transfer from $[Ru(bpy)_3]Cl_2$ to compound **1**.

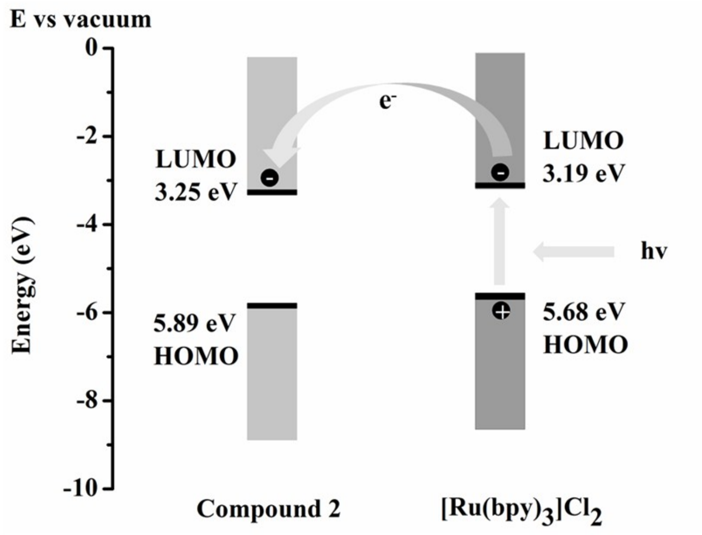


**Fig. S18** Schematic energy-level diagram showing electron transfer from $[Ru(bpy)_3]Cl_2$ to compound **2**.

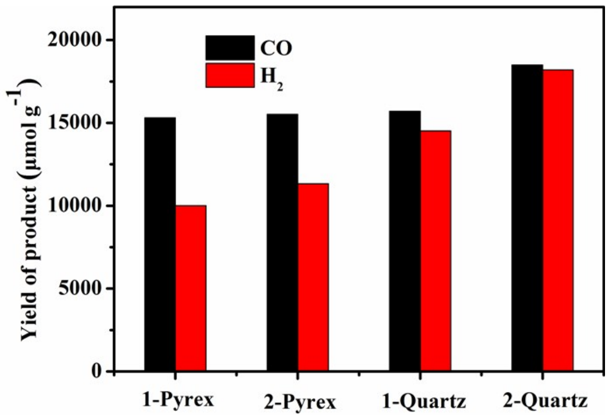


**Fig. S19** Comparison of the yields (CO and $H_2$) of compounds **1** and **2** using quartz tube and pyrex tube, respectively.

**Table S1** Crystal data and structure refinements for **1** and **2.**

| | **1** | **2** |
|---|---|---|
| Empirical formula | $C_8H_{20}Cl_{1.33}Co_{2.67}N_{12}O_{44}SiW_{12}$ | $C_{12}H_{36}Cl_2Co_3N_{18}O_{49}SiW_{12}$ |
| Formula weight | 3415.25 | 3698.57 |
| Temperature/K | 296.15 | 296.15 |
| Crystal system | cubic | triclinic |
| Space group | I*4-3d* | *P*-1 |
| *a*/Å | 25.1342(4) | 12.7994(10) |
| *b*/Å | 25.1342(4) | 13.1541(11) |
| *c*/Å | 25.1342(4) | 18.1961(15) |
| *α*/° | 90 | 92.8590(10) |
| *β*/° | 90 | 90.2200(10) |
| *γ*/° | 90 | 95.7360(10) |
| Volume/$Å^3$ | 15878.0(8) | 3044.3(4) |
| *Z* | 12 | 2 |
| $D_{calcd}$($g \cdot cm^{-3}$) | 4.301 | 4.035 |
| $\mu$/$mm^{-1}$ | 26.971 | 23.585 |
| *F*(000) | 18008.0 | 3286.0 |
| 2θ Range /° | 3.97-50.076 | 3.116-49.998 |
| Reflections collected | 43958 | 17621 |
| Independent reflections | 2346 | 10690 |
| Good on $F^2$ | 1.017 | 0.980 |
| $R_1$ [I>=2σ (I)][a] | 0.0235 | 0.0406 |
| w$R_2$ [I>=2σ (I)][b] | 0.0547 | 0.0851 |
| $R_1$[a] (all data) | 0.0261 | 0.0597 |
| w$R_2$[b] (all data) | 0.0563 | 0.0940 |
| $R_{int}$ | 0.0806 | 0.0365 |

[a]$R_1 = \Sigma||F_0| - |F_c||/\Sigma|F_0|$. [b]$wR_2 = [\Sigma w(F_0^2 - F_c^2)^2/\Sigma w(F_0^2)^2]^{1/2}$.

**Table S2** Comparison of the photocatalytic performance of compounds **1** and **2** with that of g-$C_3N_4$ and its derivatives

| catalyst | CO (μmol $g^{-1}$) | $H_2$ (μmol $g^{-1}$) | CO (μmol $g^{-1}$ $h^{-1}$) | $H_2$ (μmol $g^{-1}$ $h^{-1}$) | Time | Ref |
|---|---|---|---|---|---|---|
| **1** | 15705 | 14523 | 5235 | 4841 | 3h | This work |
| **2** | 18501 | 18199 | 6167 | 6066 | 3h | This work |
| Mo/$C_3N_4$ | 105 | 224 | 18 | 37 | 6h | 1 |
| $Co_4$@g-$C_3N_4$ | 896 | 53.2 | - | - | 10 | 2 |
| rGO/$Ag_2S$/CN | 178.05 | - | - | - | 8h | 3 |


1. R. Y. Zhang, P. H. Li, F. W, L. Q. Ye, A. Gaurc, Z. Huang, Z. Y. Zhao, Y. Bai, Y. Zhou. Applied Catalysis B: Environmental, 2019, 250, 273–279.
2. J. Zhou, W. C. Chen, C. Y. Sun, L. Han, C. Qin, M. M. Chen, X. L. Wang, E. B. Wang, Z. M. Su. ACS Appl. Mater. Interfaces, 2017, 9, 11689−11695.
3. X. Li, D. Shen, C. Liu, J. Z. Li, Y. J. Zhou a, X. H. Song, P. W. Huo, H. Q. Wang, Y. S. Yan. Journal of Colloid and Interface Science, 2019, 554, 468–478.


**Table S3** Comparison of the photocatalytic activities of **1** and **2** with the reported heterogeneous materials working in pure $CO_2$ at 1.0 atm.

| Catalyst | [Catalyst] | Light source (nm) | Photosensitizer | Solvent | Products | $TON_{CO}$ | Time | Reference |
|---|---|---|---|---|---|---|---|---|
| **1** | 0.3μM | 420 | $[Ru(bpy)_3]Cl_2·6H_2O$ | TEOA/MeCN/$H_2O$ | CO, $H_2$ | 52.35 | 3h | This work |
| **2** | 0.3μM | 420 | $[Ru(bpy)_3]Cl_2·6H_2O$ | TEOA/MeCN/$H_2O$ | CO, $H_2$ | 61.67 | 3h | This work |
| ReP:CoP | 0.05μM | 400 | / | 1,3-dimethyl-2-phenyl-1,3-dihydrobenzimidazole/DMF/$H_2O$ | CO, $H_2$ | 70 | 10h | 4 |
| Co-ZIF-9 | 0.8 μM | 420 | $[Ru(bpy)_3]^{2+}$ | TEOA/MeCN/$H_2O$ | CO, $H_2$ | 89.6 | 0.5h | 5 |
| $[Co^{II}(TPA)Cl]Cl$ | 0.005 mM | 460 | $Ir(ppy)_3$ | TEA/$CH_3CN$ | CO, $H_2$ | 900 | 70h | 6 |
| $CoCl_2·6H_2O$ | 0.17 mM | 420 | $[Ru(bpy)_3]^{2+}$ | EMIM][$BF_4$]/$H_2O$/TEOA | CO, $H_2$ | 35 | 2h | 7 |
| $[Co(bpy)_3]^{2+}$ | 0.2 mM | 420 | CdS | [EMIM][$BF_4$]/TEOA/$H_2O$ | CO, $H_2$ | 44 | 2h | 8 |
| $[Co(L-N_5)]^{2+}$ | 0.05 mM | 460 | $Ir(ppy)_3$ | $CH_3CN$/ TEA | CO | 270 | 22h | 9 |
| Co-$(bpy)_3Cl_2$/g-CN | 1 μM | 420 | / | MeCN/TEOA/$CoCl_2$/bpy | CO, $H_2$ | 4.3 | 2h | 10 |


**References**
4. J. S. Lee, D. I. Won, W. J. Jung, H. J. Son, C. Pac, S. O. Kang, *Angew. Chem. Int. Ed.*, 2017, **56**, 976 –980.
5. S. B. Wang, W. S. Yao, J. L. Lin, Z. X. Ding, X. C. Wang, *Angew. Chem. Int. Ed.*, 2014, **53**, 1034 –1038.
6. S. L. F. Chan, T. L. Lam, C. Yang, S. C. Yan, N. M. Cheng, *Chem. Commun.*, 2015, **51**, 7799.
7. J. L. Lin, Z. X. Ding, Y. D. Hou, X. C. Wang, *Scientific Reports.*, 2013, **3**, 1056.
8. J. L. Lin, Y. D. Hou, Y. Zheng, X. C. Wang, *Chem. Asian J.*, 2014, **9**, 2468.
9. L. J. Chen, Z. G. Guo, X. G. Wei, C. Gallenkamp, J. Bonin, E. Anxolabéhère-Mallart, K. C. Lau, T. C. Lau, M. Robert, *J. Am. Chem. Soc.*, 2015, **137,** 10918−10921.
10. J. L. Lin, Z. M. Pan, X. C. Wang, *ACS Sustainable Chem. Eng.*, 2014, **2**, 353−358.

**Table S4** Comparison of the cost of compounds **1** and **2** with other materials

| Entry | material | price (yuan/g) | material | Price (yuan/g) | material | Price (yuan/g) | Ref. |
|---|---|---|---|---|---|---|---|
| **1**, **2** | $CoCl_2·6H_2O$ | 209/500 | $H_4SiW_{12}O_{40}·2H_2O$ | 74/25 | 1,2,4-triazole | 202/25 | This work |
| $Co_4$@g-$C_3N_4$ | g-$C_3N_4$ | 990/0.2 | $H_3O_{40}PW_{12}$ | 90/25 | $Co(NO_3)_2$ | 368/500 | 2 |
| POM-Pt NPs@$NH_2$-silica. | aluminum chloride hexahydrate | 69/500 | 2-aminoterephthalic acid | 295/25 | $H_2PtCl_6$ | 1429/10 mL | 11 |
| | $H_3PW_{12}O_{40}$ | 90/25 | | | | | |
| $TiO_2$-POM | $TiO_2$ powders | 89/100 | $H_3O_{40}PW_{12}$ | 90/25 | $H_4SiW_{12}O_{40}·2H_2O$ | 74/25 | 12 |
| | $H_3PMo_{12}O_{40}$ | 79/25 | | | | | |


11. W. W. Guo, H. J. Lv, Z. Y. Chen, K. P. Sullivan, S. M. Lauinger, Y. N. Chi, J. M. Sumliner, T. Q. Lian, C. L. Hill. *J. Mater. Chem. A*, 2016, **4**, 5952.

12. H. Zheng, C. H. Wang, X. T. Zhang, Y. Y. Li, H. Ma, Y. C. Liu. Applied Catalysis B: Environmental, 2018, **234**, 79–89.


**Table S5** Fitted lifetimes of the fluorescence decay profiles of photosensitizer in the absence and presence of 0.5 mg **1** and 0.5 mg **2**.

| **Photocatalyst** | **$A_1$** | **$\tau_1$** |
|---|---|---|
| $[Ru(bpy)_3]Cl_2·6H_2O$ | 2315.95 | 1.21 |
| Compound 1 | 2075.58 | 1.08 |
| Compound 2 | 1714.93 | 1.01 |

**Table S6** Optical band gap $E_{VB}$ and $E_{CB}$ of catalysts **1** and **2.**

| **Compounds** | **$E_g$ (eV)** | **$E_{VB}$ (eV)** | **$E_{CB}$ (eV)** |
|---|---|---|---|
| Compound **1** | 2.90 | 1.84 | -1.06 |
| Compound **2** | 2.64 | 1.45 | -1.19 |

**Table S7** Comparison of the energy of Co-POMs and $[Ru(bpy)_3]Cl_2$**.**

| Sample | **$E_{VB}$** | **$E_{HOMO}$** | **$E_{CB}$** | **$E_{LUMO}$** |
|---|---|---|---|---|
| $[Ru(bpy)_3]Cl_2$ | 1.24 | -5.68 | -1.25 | -3.19 |
| Compound **1** | 1.84 | -6.28 | -1.06 | -3.38 |
| Compound **2** | 1.45 | -5.89 | -1.19 | -3.25 |